Nonlinear laser spectroscopy and magneto-optics

Dmitry Budker,[a] Donald J. Orlando,[b] and Valeriy Yashchuk[c]
Department of Physics, University of California, Berkeley, Berkeley, California 94720-7300

(Received 13 August 1998; accepted 9 November 1998)

An experiment on nonlinear laser spectroscopy and magneto-optics at the Advanced Undergraduate Laboratory at Berkeley is described. The experiment consists of three parts. In the first part, students learn to operate a diode laser system and characterize its performance using a Fabry–Perot spectrum analyzer. In the second part, Doppler-broadened laser-induced fluorescence and Doppler-free saturated absorption spectra of the rubidium D_2 line (780 nm) are recorded and analyzed. Finally, in the third part of the experiment, which we describe in greater detail, the near-resonant magneto-optical rotation is investigated. Nonlinear light-atom interaction leads to spectacular manifestations of the resonant Faraday effect—polarization plane rotation in a magnetic field applied along the direction of light propagation radically different from the linear case. In particular, narrow ($\sim$30 Hz) effective line widths are observed in this experiment corresponding to a rotation enhancement by some seven orders of magnitude compared to the linear Faraday rotation.

I. INTRODUCTION

In this paper, we describe a new experiment at the Advanced Undergraduate Laboratory (Physics 111) at Berkeley. The goal of the experiment is to introduce students to several modern techniques in laser spectroscopy. Ever since tunable lasers became widely available in the early seventies, laser spectroscopy has played an exceedingly important role in both fundamental research[1] and a variety of applications in chemistry, environmental research, material science, biology, and medicine.[2,3] However, experiments using tunable lasers have started to appear in undergraduate physics laboratories only relatively recently (see, e.g., Refs. 4–6) after the technology for making inexpensive tunable single-frequency diode lasers was developed.

In this experiment, we use a relatively simple setup to introduce students to the basics of diode lasers, to Doppler-free high-resolution spectroscopy, and to nonlinear magneto-optics. While the former two of these topics have been discussed in the past,[4] nonlinear magneto-optics, illustrated here by the nonlinear Faraday effect, is being introduced to an undergraduate laboratory, as far as we know, for the first time. The nonlinear Faraday effect is a spectacular phenomenon of considerable recent theoretical and experimental interest (see, e.g., Refs. 7–12 and references therein). Recent advances in nonlinear magneto-optics related to the observations of long-lived atomic alignment[13] open new possibilities of applying this technique to precision magnetometry and fundamental measurements, including sensitive searches for linear Stark shifts in an atom,[14] which could arise due to a violation of both parity- and time-reversal invariance.[15] The underlying physical mechanisms are closely related to traditional optical pumping and saturation spectroscopy on the one hand, and to many other nonlinear optical phenomena of current research interest, including electromagnetically induced transparency,[16] coherent dark resonances,[17,18] phaseonium,[19] etc., on the other.

This paper is structured as follows. In Sec. II, we give an elementary discussion of the linear and nonlinear Faraday effects, pointing out their relation to the linear and nonlinear absorption. The general experimental arrangement is described in Sec. III. Results on Doppler limited laser-induced fluorescence and high-resolution saturation spectroscopy are briefly summarized in Sec. IV. Section V is devoted to a description of experimental observations of nonlinear Faraday rotation, which illustrate the existence of several distinct nonlinear mechanisms that manifest themselves in optical rotation. This part of the experiment is described in greater detail. The most important result is observation of long-lived ground-state atomic coherence giving rise to narrow features in the magnetic field dependence of the nonlinear optical rotation with effective widths $\approx$30 Hz. (The narrowest observed width in experiments of this kind is $\approx$1.3 Hz.[13]) Finally, conclusions are drawn in Sec. VI. Appendices A and B are devoted to description of details of the construction of a simple scanning confocal Fabry–Perot spectrum analyzer and the magnetic shield and coil.

II. LINEAR AND NONLINEAR MAGNETO-OPTICAL ROTATION

The Faraday effect[20] is the rotation of the plane of linear light polarization by a medium subject to a magnetic field applied in the direction of light propagation. In 1898, Macaluso and Corbino,[21] studying absorption spectra of the alkali atoms in the presence of magnetic fields, discovered that the Faraday effect in the vicinity of resonance absorption lines also has a distinct resonant character.

The essence of the Macaluso–Corbino effect can be illustrated by considering the case of an $F=1\rightarrow F'=0$ transition (Fig. 1), where F and F' are the total angular momenta. Linearly polarized light incident on the sample can be resolved into two counter-rotating circular components $\sigma^{\pm}$. In the absence of a magnetic field, the $M=\pm 1$ sublevels are degenerate and the optical resonance frequencies for σ^+ and σ^- coincide. The refractive index associated with the atomic medium (the dispersion curve) is sketched in Fig. 2. It is the same for the two circular components. When a magnetic field is applied, however, the Zeeman shifts lead to a difference between the resonance frequencies for the two circular polarizations. This displaces the dispersion curves for the two polarizations as shown in Fig. 2. A characteristic width of these dispersion curves, Γ, corresponds to the spectral width of an absorption line, which under typical experimental conditions in a vapor cell is dominated by the Doppler

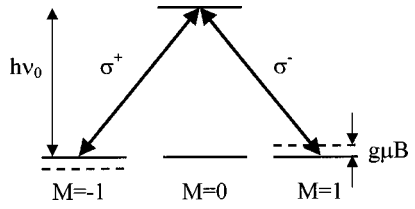

Fig. 1. An $F=1\rightarrow F'=0$ atomic transition. In the presence of a longitudinal magnetic field, the Zeeman sublevels of the ground state are shifted in energy by $g\mu B\cdot M$. This leads to a difference in resonance frequencies for left- and right-circularly polarized light ($\sigma^{\pm}$).

width and is on the order of 1 GHz for optical transitions. The difference between n_+ and n_- is shown in the lower part of Fig. 2. It leads to a difference in phase velocities of the two circular components of light and, as a result, the plane of polarization rotates through an angle:

$$\varphi=\pi(n_+-n_-)\frac{l}{\lambda}. \tag{1}$$

Here l is the length of the sample, and λ is the wavelength of light. In general, in addition to there being a difference in refractive index for the two circular polarizations (circular birefringence), there is also a difference in absorption (circular dichroism). Thus, linear light polarization before the sample generally evolves into elliptical polarization after the sample.

For nearly monochromatic light (i.e., light with spectral width much smaller than the transition width), and for zero frequency detuning from the resonance, the optical rotation in the sample as a function of magnetic field can be estimated from Eq. (1) as

$$\varphi\sim\frac{2g\mu B/\hbar\Gamma}{1+(2g\mu B/\hbar\Gamma)^2}\cdot\frac{l}{l_0}. \tag{2}$$

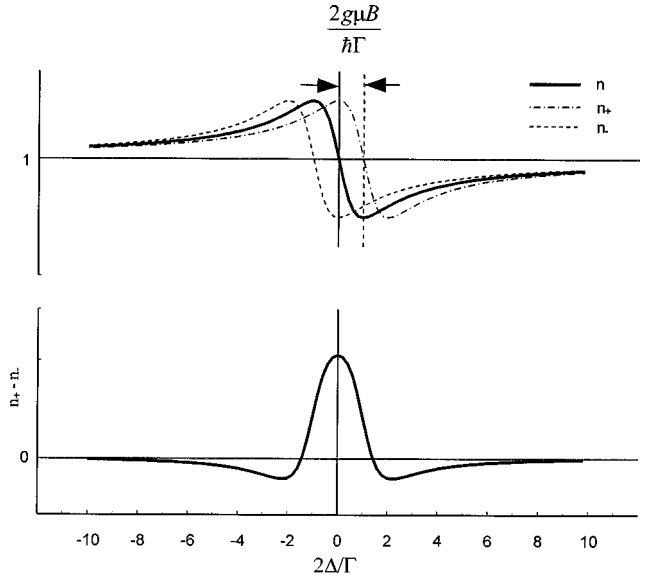

Fig. 2. The dependence of the refractive index on light frequency detuning Δ in the absence (n) and in the presence ($n_{\pm}$) of a magnetic field. Shown is the case of $2g\mu B=\hbar\Gamma$ and a Lorentzian model for line broadening. The lower curve shows the difference in refractive index for the two circular polarization components. This is the characteristic spectral profile of Macaluso–Corbino optical rotation.

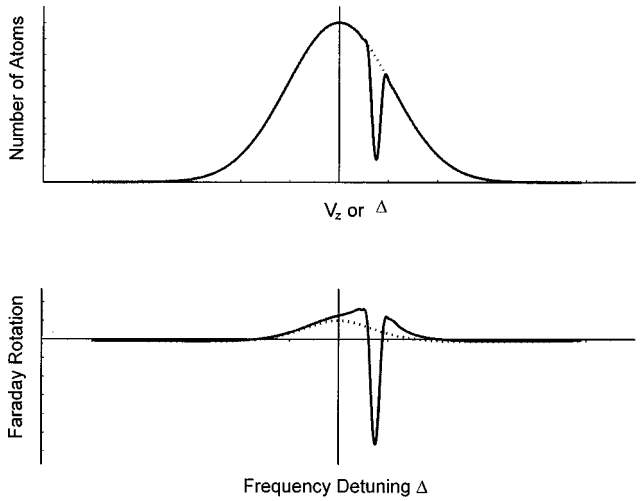

Fig. 3. The hole-burning effect in nonlinear Faraday rotation. This figure assumes $|2g\mu B|\ll\hbar\Gamma$. Monochromatic laser light produces a Bennett hole in the velocity distribution of atoms in the lower state of the optical transition (upper trace). The Faraday rotation produced by atoms with such velocity distribution can be seen as rotation produced by unperturbed distribution minus the rotation that would have been produced by atoms removed by optical pumping (lower trace).

Here l_0 is the absorption length. In this estimate we use the fact that near an absorption line, the amplitude of each dispersion curve (Fig. 2) is comparable to the resonance value of the imaginary part of the complex refractive index responsible for absorption. The Lorentzian model for line broadening is assumed. Gaussian and Voigt models (see, e.g., Ref. 3), which most accurately describe a Doppler-broadened line, lead to qualitatively similar results. The dependence of the optical rotation on the magnitude of the magnetic field has a characteristic dispersionlike shape: φ is linear with B at small values of the field, peaks at $2g\mu B\sim\pm\hbar\Gamma$, and falls off in the limit of large fields. This elementary discussion summarizes the linear (in light power) resonant Faraday rotation.

It is well known that in nonlinear spectroscopy (which takes advantage of the medium's susceptibility dependence on the light field) it is possible to achieve much narrower line widths than in linear spectroscopy. In Faraday rotation, this leads to dramatic differences in the spectrum and magnitude of the rotation compared to the linear case. In particular, the small-field rotation can be enhanced by many orders of magnitude. This is because the small-field optical rotation is inversely proportional to Γ [cf. Eq. (2)].

The simplest nonlinear effect is ''hole burning.'' A pump laser beam produces a so-called Bennett hole—a dip in the velocity distribution of the ground state atoms. In saturation spectroscopy, this narrow structure is analyzed with a probe laser beam, allowing spectral resolution determined by the width of the hole.[2,3] Hole burning is also the simplest nonlinear effect leading to enhanced Faraday rotation. The hole in the atomic velocity distribution due to velocity-selective optical pumping is shown on the upper trace in Fig. 3. The hole width corresponds to the natural linewidth of the transition, typically $\sim$1–10 MHz (here we are assuming light bandwidth much smaller than the natural width). The Faraday rotation produced by atoms with such velocity distribution can be thought of as rotation produced by the Doppler-distributed atoms without the hole minus the rotation that

would have been produced by the pumped out atoms. This is illustrated on the lower trace of Fig. 3. Because the hole width is much narrower than the Doppler width, we have a correspondingly larger small field rotation [see Eq. (2)], which is also of opposite sign compared to the linear effect.

In many experiments, instead of using separate pump and probe laser beams, one beam is used both to produce the hole and to probe the optical rotation. This corresponds to always probing the peak of the nonlinear effect. Thus, when the laser frequency is tuned across the resonance, the optical rotation exhibits broad spectral profile which looks like a Doppler-broadened absorption curve and has nonzero integral rotation, and not the characteristic Macaluso–Corbino profile with zero integral rotation shown in Fig. 2.

Even narrower widths are due to the coherence effects in nonlinear spectroscopy.[8,17] These effects may lead to significantly higher small-field optical rotation than the hole-burning effect. Consider again atoms with total angular momentum $F=1$ which are not aligned initially and linearly polarized laser light with frequency corresponding to an $F=1\rightarrow F'=0$ transition. To analyze the nonlinear light–atom interaction, it is convenient to view the atoms as being in an incoherent mixture of the following states: $|M=0\rangle$, $1/\sqrt{2}(|M=1\rangle\pm|M=-1\rangle)$. The first of these states can be excited to the $F'=0$ state only by **z**-polarized radiation (**z**-absorbing state), while it is decoupled from **x**- and **y**-polarized light. Similarly, the other two states (which are coherent superpositions of the $|M=\pm1\rangle$ Zeeman sublevels) are **y**- and **x**-absorbing states, respectively. Suppose the laser light is polarized in the **x** direction. Optical pumping by this light leads to a depletion of the **x**-absorbing state. If the light power is sufficiently high, the medium becomes transparent for the **x**-polarized radiation, leaving atoms in the **y**- and **z**-absorbing states. This process is known as coherent population trapping[17] because, as a result of optical pumping by linearly polarized light, atoms in the $M=\pm1$ substates are not completely pumped out as would seem to be the case at first glance (see Fig. 1), but largely remain in a ''dark'' coherent superposition.

Atoms in this dark state do not interact with light of the same polarization as pump light. However, they can still absorb and refract light of an orthogonal polarization. This is a manifestation of atomic alignment.[22] Optical pumping into a dark state is a particular case of alignment. In general, alignment can exist even when there is no dark state (i.e., for $F\rightarrow F+1$ transitions[23]). This actually applies to the experimental results in Rb discussed below. An ensemble of aligned atoms constitutes a medium with linear dichroism and birefringence. The birefringence turns out not to be important for the coherence effect because the refractive index is unity on resonance.

In the presence of a magnetic field, the atomic alignment axis created by the coherent population trapping precesses around the direction of the field with the Larmor frequency (precession of atomic alignment in a magnetic field is explained in detail, e.g., in Ref. 24). The effect of this precession on the light polarization can be understood if one thinks of the atomic medium as a layer of polarizing material like a Polaroid film, see Fig. 4. It is easy to see that rotation of the ''polarizer'' around the z axis results in a linear polarization of light at the output of the sample which is rotated by an angle proportional to the optical density of the sample and to $\sin(2\theta)$, where θ is the angle between the transmission axis

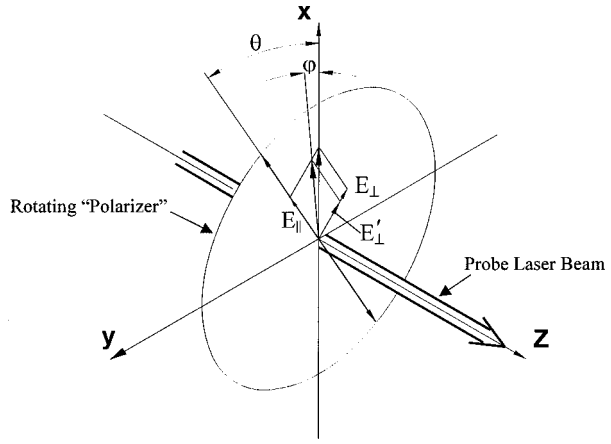

Fig. 4. An optically thin sample of aligned atoms precessing in a magnetic field can be thought of as a thin rotating Polaroid film, which is transparent to light polarized along its axis ($E_{\parallel}$), and slightly absorbent for the orthogonal polarization ($E_{\perp}$). $E_{\parallel}$ and $E_{\perp}$ are the light electric field components. The effect of such a ''polarizer'' is to rotate the light polarization by an angle $\varphi\propto\sin(2\theta)$. The figure is drawn assuming a magnetic field directed along z.

of the rotated ''polarizer'' and the direction of light polarization. In order to describe optical rotation of cw laser light, one has to sum the effect of elementary ''polarizers'' produced at times $-\infty<t<0$ and to include relaxation. Using this model, one can show[12] that for sufficiently low light power and magnetic field, the rotation due to the coherence effect is once again described by Eq. (2), but now the relevant relaxation rate is that of the ground state alignment.

The two mechanisms of the nonlinear Faraday effect discussed above, the hole-burning and the coherence effect, produce narrow features (resonances) in the magnetic field dependence of the rotation with widths corresponding to their respective relaxation rates.[25] Below (Figs. 8–11), we will illustrate various contributions to the nonlinear Faraday effect using the data obtained in the Physics 111 laboratory at Berkeley.

III. EXPERIMENTAL SETUP

The diagram of the apparatus is shown in Fig. 5. A commercial external cavity diode laser system (EOSI 2010, central wavelength $\lambda\approx780$ nm, power $P\approx10$ mW) is used in this experiment.[26] The laser is tuned to the rubidium D_2 resonance, $^2S_{1/2}\rightarrow{}^2P_{3/2}$ at 780.2 nm. Small portions of the laser beam are split with beamsplitters mounted on standard 1 in. mirror mounts into various parts of the experiment. The beamsplitters are just pieces of 0.1 mm thick microscope cover glass glued to the mirror mounts (thin cover glass is used to avoid interference effects during laser scanning). The beamsplitter BS-1 directs a portion of laser light onto a scanning confocal Fabry–Perot (F-P) interferometer, which is used as a spectrum analyzer to monitor the mode structure of the laser output and to provide frequency markers. In this experiment, we use a homemade F-P interferometer, which gives comparable performance to the commercial devices, but at a small fraction of the cost. Appendix A describes the details of its mechanical design.

The beamsplitters BS-2 and BS-3 provide light beams used for the laser-induced fluorescence and Doppler-free saturation spectroscopy experiments. The fluorescence signal from Rb atoms in the vapor cell VC-1 is detected by the

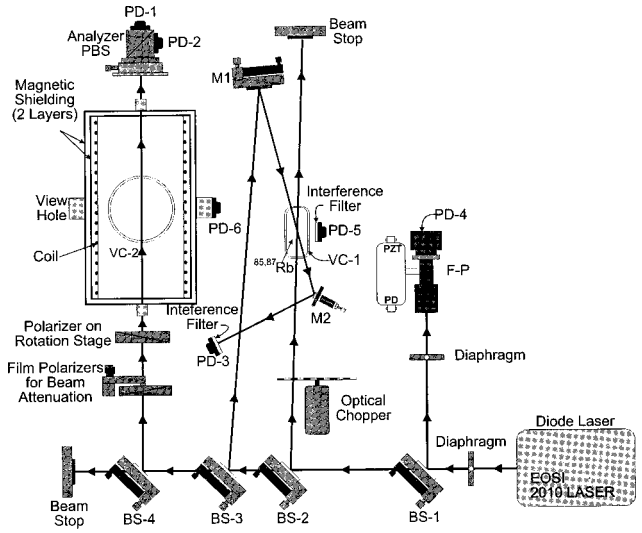

Fig. 5. Diagram of the experimental setup. BS—beamsplitters; PD—photodiodes; VC—Rb vapor cells; F-P—Fabry–Perot interferometer. The angle between the laser beams intersecting in VC-1 is greatly exaggerated.

photodiode PD-5. For the saturation spectroscopy measurement, a standard arrangement[2,3] is used. The nearly counter-propagating pump beam (provided by the beamsplitter BS-2) and the probe beam (split by BS-3) are overlapped in the vapor cell VC-1. The pump beam is interrupted with an optical chopper (SR540[27]), and the synchronous signal from the photodiode PD-3 is extracted with a lock-in amplifier (SR830 DSP[27]). The photodiodes in this experiment are equipped with 780 nm interference filters to reduce the pick-up from the room lights.

Light reflected from the beamsplitter BS-4 is used in the magneto-optics part of the experiment. This light first goes through two pieces of Polaroid film. These are used as a variable attenuator for the light power. Next, the beam goes through a precision prism polarizer and through a Rb vapor cell VC-2 installed inside a two-layer magnetic shield (Appendix B). A magnetic coil is installed inside the inner shield. This setup is used to shield the lab magnetic field and to produce a well-controlled field along the axis of the chamber. Next, the light beam is split by a polarizing beam splitter (PBS), and the two resulting beams fall onto photodiodes (PD-1 and PD-2) which detect their power P_1 and P_2. The axis of the PBS is rotated by $\pi/4$ with respect to the axis of the polarizer. This arrangement is called a balanced polarimeter. Using Malus' law for the transmission of linearly polarized light through a linear polarizer, it is easy to show that the optical rotation in the sample δ (for $\delta \ll 1$) is

$$\delta = \frac{P_1 - P_2}{2 \cdot (P_1 + P_2)}. \tag{3}$$

It is easy to show also that the balanced polarimeter is insensitive to circular dichroism of the sample—unequal absorption for the right- and left-circular polarizations, making this device appropriate for investigating optical rotation in a general situation where the light after the sample is elliptically polarized.

The control over laser frequency tuning, magnetic field scans, and data acquisition is accomplished using a personal computer with a plug-in data acquisition board[28] and software written in the LABVIEW™ environment.

IV. RESULTS ON LASER-INDUCED FLUORESCENCE AND DOPPLER-FREE SATURATION SPECTROSCOPY

In the first part of the experiment with this setup, students learn to operate the diode laser and characterize its output. Next, they observe Doppler-broadened laser-induced fluorescence spectra of Rb (Fig. 6). The laser-induced fluorescence profile on the D_2 line consists of four peaks corresponding to two ground-state hyperfine components for each of the two stable rubidium isotopes: ^{85}Rb (nuclear spin $I=5/2$, relative abundance 72%) and ^{87}Rb ($I=3/2$, 28%); the upper state hyperfine structure is unresolved.

In the next step, the Doppler-free saturation absorption spectra are recorded (Fig. 7). Here the upper state hyperfine structure is resolved. In addition to the primary hyperfine resonances, the so-called crossover resonances are also clearly seen on the figure. These resonances occur when the laser is tuned halfway between two primary resonances. They correspond to the pump and probe beam interacting with a certain velocity group via two different hyperfine tran-

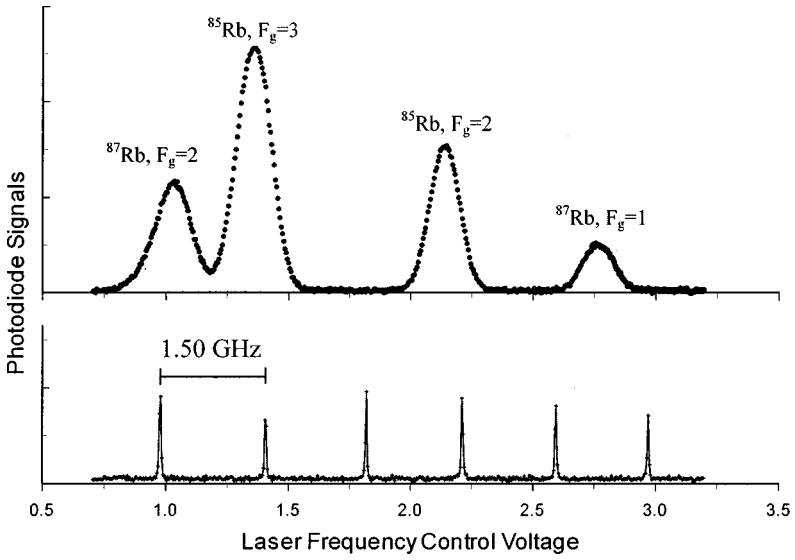

Fig. 6. Upper trace: a recording of the Doppler-broadened fluorescence spectrum of the Rb D_2 line (signal from PD-5 on Fig. 5). Lower trace: a transmission spectrum of the Fabry–Perot spectrum analyzer providing frequency markers separated by 1.5 GHz (signal from PD-4). The Fabry–Perot peak heights appear to vary mainly because the frequency sampling interval is comparable to the peak width.

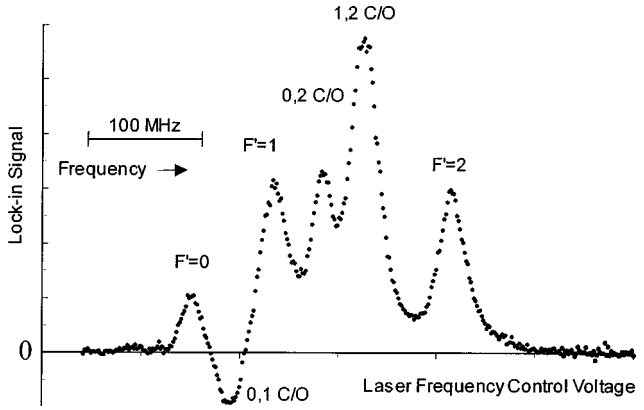

Fig. 7. An example of a saturated absorption spectrum: the $F_g=1\rightarrow F'$ component of the D_2 line for ^{87}Rb. The upper state hyperfine structure is resolved. The horizontal scale is expanded $\times 20$ with respect to Fig. 6. C/O: crossover resonances. As discussed in the text, the 0,1 crossover under the conditions of this scan is of opposite sign relative to the other peaks. Light power for both the pump and the probe beam is ~0.1 mW; beam diameters are ~2 mm.

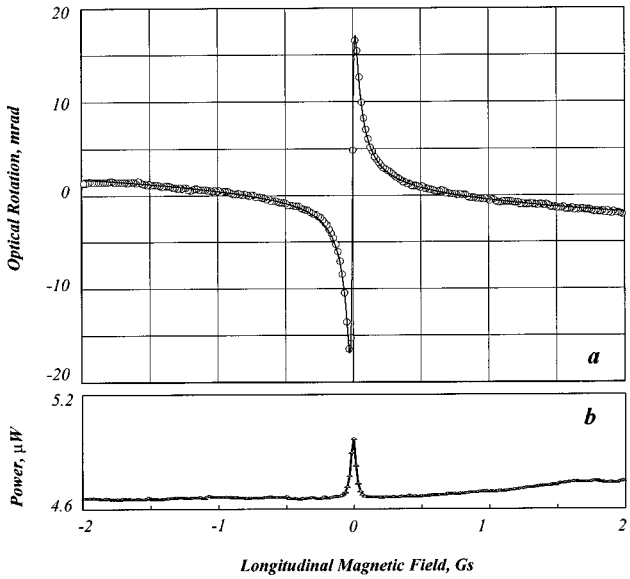

Fig. 8. Nonlinear Faraday rotation (a) and transmitted light power (b) recorded with an uncoated cell. The laser is tuned to the center of $F_g=2\rightarrow F'$ component of the D_2 line for ^{85}Rb. The overall slope of the rotation curve is due to the hole-burning effect. The central feature is the coherence effect. Its width is determined by the atoms' transit time through the laser beam (~10 mm diam.). The transmission curve shows a dark resonance at zero magnetic field.

sitions with a common lower level. It is curious to note that the peak corresponding to the 0,1 crossover on Fig. 7 is inverted under the conditions of this experiment. Similar peculiarities in the saturated absorption lineshapes have been studied previously.[29] They are related to interplay between depopulation and repopulation optical pumping in the presence of the laboratory magnetic fields (not shielded for this part of the experiment). Comparison of the fluorescence spectra to the saturated absorption spectra illustrates the striking advantage in spectral resolution of the latter technique. This part of the experiment is similar in its scope (although quite different in the details of realization) to other advanced undergraduate experiments that have been described in the past.[4] Therefore, we omit a detailed discussion here. A partial list of issues investigated by students in this part of the Berkeley experiment includes hyperfine structure and isotope shift, spectral line broadening mechanisms (Doppler, natural, light power broadening), etc.

V. RESULTS ON NONLINEAR MAGNETO-OPTICS

These experiments were performed with two different vapor cells. One was an uncoated cylindrical cell (2.5 cm diam $\times$7.5 cm long) with a natural mixture of Rb isotopes, and the other was an 8 cm diam. paraffin-coated spherical cell with ^{85}Rb.[30] Figure 8(a) shows the magnetic field dependence of the Faraday rotation in the uncoated cell for the laser tuned near the peak of the ^{85}Rb ($F_g=2\rightarrow F'$) Doppler-broadened resonance. The overall slope in the figure is due to the hole-burning effect. This is the central part of the dispersively shaped feature with characteristic width ~10 Gs which is clipped due to the limited magnetic field scan range. Recall that even at the extremes of the available magnetic field range ($\pm$2 Gs), the contribution of the linear Faraday rotation is some three orders of magnitude smaller than that of the nonlinear effect. The narrow structure in Fig. 8(a) is due to the coherence effect. Its characteristic width ~40 mGs corresponding to $\Gamma\sim 2\pi\cdot 20$ kHz is determined by the atoms' transit time through the laser beam ($\Gamma\sim v_t/d$, where $v_l\approx 2.5\times 10^4$ cm/s is the thermal velocity of Rb atoms, and $d\approx 1$ cm is the laser beam diameter). The aligned atoms fly out of the laser beam, while ''fresh'' atoms from the volume of the cell are replacing them. This effectively provides for the alignment relaxation. The experimental magnetic field dependence of the Faraday rotation is fit with a theoretical lineshape that consists of two terms of the form of Eq. (2). Their widths and amplitudes correspond to the two contributions to the optical rotation discussed above. The fitting curve is shown in the figure along with the experimental data. Figure 8(b) shows the recording of the light power transmitted through the cell. The slow variation on this curve is due to a minute laser power drift over the period of the scan (~ 1 min), while the sharp peak in transmission is the so-called ''dark resonance,'' [17,31] which is another manifestation of the coherence effect. The origin of this resonance can be understood in the physical picture used above to describe optical rotation. The precession of the light-induced atomic alignment (the dichroic ''polarizer'') causes changes in the light transmission through the medium. Depending on the angular momentum values of the atomic states involved in the transition, the resonance could be either dark [as in Fig. 8(b)] or bright. A dark resonance corresponds to a decrease in absorption at zero magnetic field. Bright resonances occur for closed $F_g\rightarrow F'=F_g+1$ transitions where optical pumping leads to increased absorption rather than bleaching.[23]

The coherence effect with effective relaxation due to atoms' transit through the laser beam gives a small-field rotation enhancement of some four orders of magnitude compared to the linear case. Even so, a considerable further enhancement is possible. One way to achieve this is to increase the diameter of the laser beam, or to use separated pump and probe laser beams.[10]

An elegant method to decrease the effective alignment relaxation rate is to use cells with an anti-relaxation coating on the inner walls. With an appropriate coating, it takes many alkali atom collisions with the wall to destroy atomic

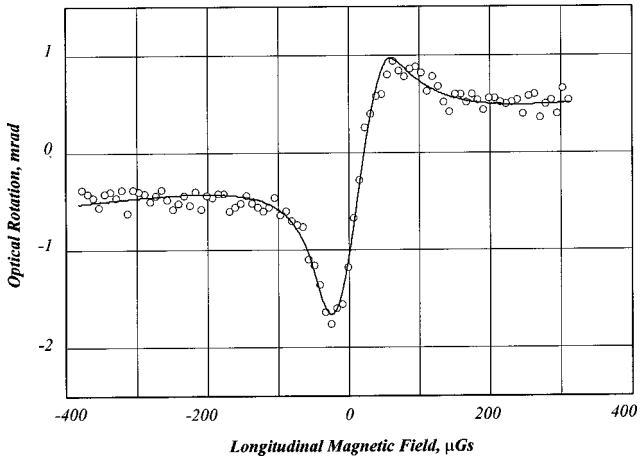

Fig. 9. The narrow nonlinear optical rotation feature recorded with a coated cell. Its origin is related to preservation of alignment in wall collisions. The laser was tuned to the center of $F_g=3$ component of the D_2 line for ^{85}Rb. The longitudinal magnetic field scan range is 5000 times smaller that on Fig. 8. The solid line represents a fit to a model incorporating the effect of residual transverse fields. The data was taken by undergraduate students A. Sushkov and M. W. Wu.

polarization.[32] Application of such cells to the nonlinear Faraday effect was first demonstrated in Ref. 11. The narrowest nonlinear magneto-optical features, $\Gamma \sim 2\pi \times 1$ Hz, were recently observed in Ref. 13. In that work, a highest-quality cell[33] with a coating that can support many thousand wall-collisions before an alkali atom loses Zeeman coherence was used along with a sophisticated magnetic shielding and residual field compensation system.

These nonlinear magneto-optics effects are also observed in the present undergraduate experiment with the coated cell. In such a cell, one observes the features similar to those in Fig. 8, however, an additional much narrower feature not present for the uncoated cell is revealed by a detailed scan of the near-zero magnetic field region. A scan corresponding to a 5000× zoom compared to Fig. 8 of this low-field region is shown in Fig. 9. The remarkably narrow width of this resonance in the magnetic field dependence of the rotation corresponds to $\Gamma \approx 2\pi \times 30$ Hz. The alignment relaxation mechanisms contributing to this width include relaxation in wall collisions, spin exchange collisions, and light broadening.[13] The shape of the nonlinear magneto-optics feature in Fig. 9 is somewhat asymmetric. This is due to the presence of residual transverse magnetic fields of the same order of magnitude as the resonance width: $B_{\rm tr} \sim \Delta B_z \approx 60\,\mu$Gs. The magnitudes of the transverse field components extracted from the fit to a theoretical model[13] are: $|Bx| \approx 55\,\mu$Gs, $|By| \approx 13\,\mu$Gs, where x corresponds to the direction of the input light polarization. Note that the sensitivity of the nonlinear optical rotation lineshape to both longitudinal and transverse fields illustrates applicability of this technique to three-axis low-field magnetometry.

Up to now in this section we have discussed the magneto-optic effects in terms of the dependence of optical rotation on magnetic field at a fixed frequency of light. A somewhat complementary picture is obtained by studying the optical rotation spectra at fixed values of magnetic field. Figure 10 shows a series of such spectra recorded with the uncoated vapor cell at various values of the magnetic field. A recording of the vapor transmission spectrum is given for reference

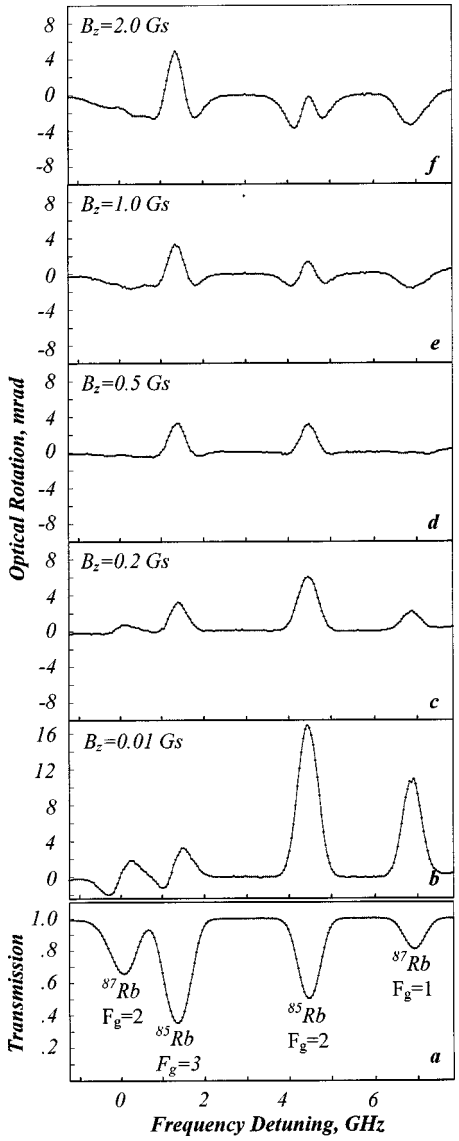

Fig. 10. Optical rotation spectra (traces b–f) at various values of the magnetic field. Input light power: $P \approx 12$ mW, beam diameter ≈8 mm. Trace a shows the vapor transmission spectrum.

as trace a in Fig. 10. Trace b shows the optical rotation spectrum at a value of the magnetic field where the rotation is dominated by the transit effect (see Fig. 8). For the lower F_g components of the line for both isotopes of Rb, the rotation peaks have the same shape as the absorption. The situation is quite different for the higher F_g components, where the rotation spectrum has dispersionlike shape. The origin of this behavior is again related to the presence of the closed transitions $F_g \rightarrow F_g+1$ in those transition groups,[12] and is closely related to the other phenomena encountered in this experiment: the peculiarities of the Doppler-free saturation spectroscopy lineshapes, and the bright resonances. Traces c–f in Fig. 10 illustrate how the rotation spectra change as the magnetic field is increased to the point where the rotation is dominated by the hole-burning effect. Unfortunately, it appears difficult to describe the details of this rather complicated spectrum without involved quantum-mechanical calculations which are beyond the scope of this work. It is interesting to note that the shown hole-burning effect spectra are qualitatively different for the two Rb isotopes.

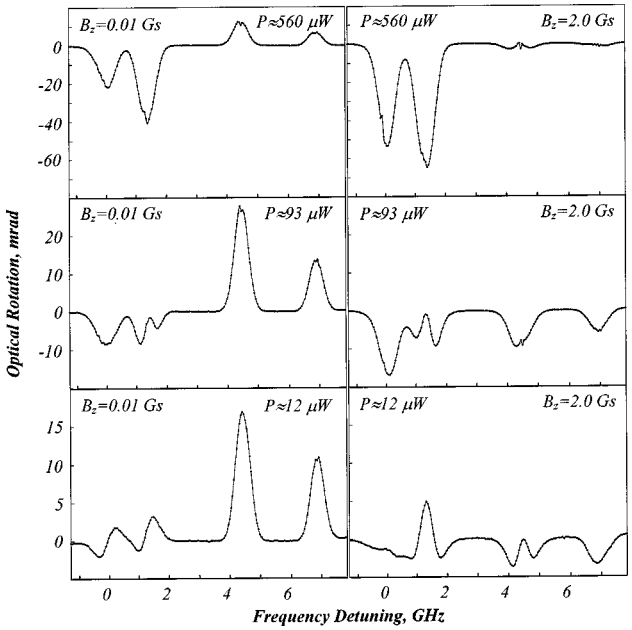

Fig. 11. Spectra of the nonlinear optical rotation for the transit effect (left column) and the hole-burning effect (right column) taken at various values of the input light power P. The laser beam diameter was ≈8 mm.

Figure 11 shows the light power dependences of the spectra for the transit effect (left column), and the hole-burning effect (right column). The detailed description of these dependences once again lies beyond the scope of this paper and the undergraduate laboratory experiment. We note, however, that the strong dependence of the optical rotation on the light power highlights the nonlinear nature of the observed magneto-optic effects. A curious observation in Fig. 11 is the presence of small sub-Doppler features in the spectra at high light power. Most likely, these are due to the presence of a light beam retro-reflected from the output window of the vapor cell, effectively producing a magneto-optic analog of the saturation spectroscopy setup with counter-propagating light beams.

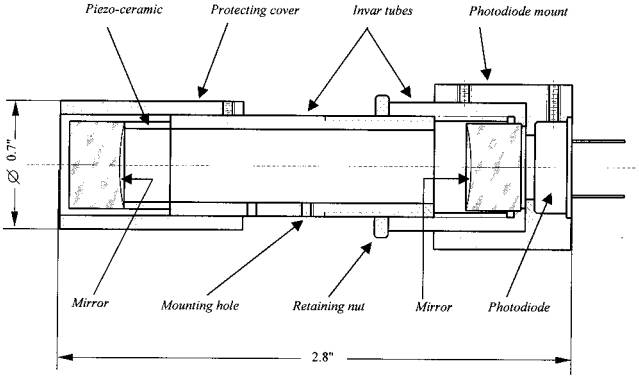

Fig. 12. Schematic of the scanning confocal Fabry–Perot spectrum analyzer.

VI. CONCLUSIONS

We have presented a new undergraduate experiment aimed at introducing students to several important topics in modern spectroscopy: diode lasers, high-resolution spectroscopy, and nonlinear magneto-optics. The relatively simple experimental setup allows us to demonstrate several nonlinear magneto-optical effects—the hole-burning effect, and the two coherence effects: the transit effect and the effect related to the preservation of atomic alignment during many wall collisions. The latter manifests itself as the sharpest feature at near-zero magnetic fields. The steep derivative of the rotation angle with respect to the magnetic field at near-zero fields corresponds to a gain of some seven orders of magnitude compared to the usual linear resonant Faraday rotation.

The same apparatus can also be used to demonstrate a number of other advanced techniques and phenomena such as laser frequency stabilization using saturation spectroscopy, light power and polarization dependence of the saturation spectroscopy signals, polarization spectroscopy,[34] magneto-optical analog of Doppler-free saturation spectroscopy (briefly mentioned above), electromagnetically induced transparency, etc.

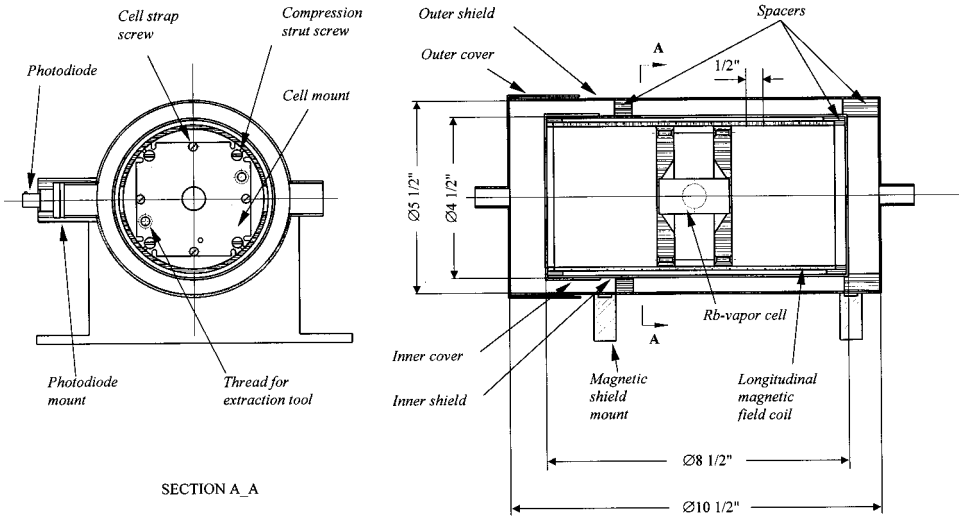

Fig. 13. Schematic of the magnetic shield and coil assembly.

ACKNOWLEDGMENTS

The authors are grateful to M. Zolotorev for most useful discussions, and to S. P. Davis, R. W. Falcone, A. T. Nguyen, and S. M. Rochester for comments on the manuscript. The first students who completed the experiment in the Spring semester of 1998 and contributed greatly to its ''debugging'' were N. Busek, M. J. Markus, S. Peters, A. Sushkov, and M. W. Wu. We thank N. Brahmal for help with graphics, M. Ambrozini, A. Waynberg, and G. Weber for machining parts of the apparatus, and J. Davis, D. Gallegos, and R. Wykoff for help with electronics. This work has been supported by NSF, Grant No. 9750873 and by ONR, Grant No. N00014-97-1-0214. We are also grateful to Stanford Research Systems for the donation of equipment used in this experiment.

APPENDIX A: THE CONFOCAL FABRY–PEROT SPECTRUM ANALYZER

Fabry–Perot spectrum analyzers are available commercially, but their cost may be prohibitively high for an undergraduate laboratory. We have constructed a simple spectrum analyzer (Fig. 12) which is a variation on a design used by many research groups (for other confocal Fabry–Perot interferometer designs and undergraduate experiments based on such interferometers, see, e.g., Ref. 5 and references therein). Its free spectral range is 1.50 GHz. This instrument shows performance (finesse, stability, etc.) more than adequate for the current application and is relatively inexpensive (total cost$<$\$1000, the most expensive item being the mirrors).

The body of the interferometer is constructed of two fine-threaded invar (a low thermal expansion alloy) pipes. One pipe threads into the other, allowing accurate adjustment of the mirror separation necessary for achieving the confocal condition. A standard concave mirror (reflectivity$\approx$98%, radius 5 cm) is glued directly to one of the pipes. The second identical mirror is glued to a piezo-ceramic hollow cylinder,[35] which, in turn, is glued to the second invar pipe. Care is taken to avoid electrically shorting the metal-coated inner and outer walls of the piezo-ceramic cylinder to the invar pipe. Application of voltage between the walls of the piezo-ceramic tube displaces the mirror, providing frequency tuning of the interferometer (typically, several free spectral ranges per 100 V). Fine adjustment of the mirror separation is accomplished while scanning either the interferometer or the laser and minimizing the width of the observed transmission peaks. Once the confocal separation between the mirrors is found, it can be locked by tightening the retaining nut.

APPENDIX B: THE MAGNETIC SHIELD AND COIL

Both layers of the magnetic shield (Fig. 13) were manufactured out of a 0.04 in. thick sheet of the high magnetic permeability CONETIC-AA alloy.[36] After manufacturing, the shields were annealed in a hydrogen atmosphere. Longitudinal magnetic field is created inside the inner shield by a magnetic coil wound on a plastic bobbin. In order to reduce the transverse components of the field, the coil is wound in a pattern in which the axial component of the current is compensated. The separations between the coil and the lids of the inner shield are equal to one-half of the separation between the adjacent turns in the coil. This is done to maximize the field homogeneity—in this arrangement the coil and its images form an infinite solenoid. The vapor cell is mounted inside the bobbin using a delrin mount fixed in place by tightening the compression strut screws.

[a]Electronic mail: budker@socrates.berkeley.edu
[b]Electronic mail: phylabs@socrates.berkeley.edu
[c]Electronic mail: yashchuk@socrates.berkeley.edu

[1]This point is clearly illustrated, for example, by the discovery and subsequent precision work on parity violation in atoms [for a recent review, see M. A. Bouchiat and C. Bouchiat, ''Parity violation in atoms,'' Rep. Prog. Phys. **60** (11), 1351–1394 (1997)], and by several Nobel prizes awarded for the work in this field, including the ones in 1997 for the development of laser trapping and cooling. [See the Nobel lectures by S. Chu, ''The manipulation of neutral particles,'' Rev. Mod. Phys. **70** (3), 685–706 (1998); C. N. Cohen-Tannoudji, ''Manipulating atoms with photons,'' *ibid.* **70** (3), 707–719 (1998); W. Phillips, ''Laser cooling and trapping of neutral atoms,'' *ibid.* **70** (3), 721–741 (1998).]

[2]S. Svanberg, *Atomic and Molecular Spectroscopy. Basic Aspects and Applications* (Springer-Verlag, New York, 1992).

[3]W. Demtröder, *Laser Spectroscopy* (Springer-Verlag, New York, 1996).

[4]K. B. MacAdam, A. Steinbach, and C. Wieman, ''A narrow-band tunable diode laser system with grating feedback, and a saturated absorption spectrometer for Cs and Rb,'' Am. J. Phys. **60**, 1098–1111 (1992); D. W. Preston and C. E. Wieman, ''Doppler-free saturated absorption spectroscopy: laser spectroscopy,'' advanced laboratory write-up (09/1994; unpublished), available from D. W. Preston, e-mail: dpreston@csuhayward.edu; D. W. Preston, ''Doppler-free saturated absorption: laser spectroscopy,'' Am. J. Phys. **64**, 1432–1436 (1996).

[5]K. G. Libbrecht, R. A. Boyd, P. A. Willems, T. L. Gustavson, and D. K. Kim, ''Teaching physics with 670 nm diode lasers—construction of stabilized lasers and lithium cells,'' Am. J. Phys. **63**, 729–737 (1995); R. A. Boyd, J. L. Bliss, and K. G. Libbrecht, ''Teaching physics with 670 nm diode lasers—experiments with Fabry-Perot cavities,'' Am. J. Phys. **64** (9), 1109–1116 (1996).

[6]I. M. Beterov, A. V. Dudnikov, V. G. Volkov, I. I. Ryabtsev, and V. M. Entin, ''Some applications of tunable diode lasers in atomic physics,'' Siberian Journal of Physics **1**, 41–56 (1997).

[7]L. M. Barkov, D. Melik-Pashayev, and M. Zolotorev, ''Nonlinear Faraday Rotation in Samarium Vapor,'' Opt. Commun. **70** (6), 467–472 (1989).

[8]W. Gawlik, ''Optical Nonlinearity and Atomic Coherences,'' in *Modern Nonlinear Optics, Part 3*, edited by M. Evans and S. Kielich, Advances in Chemical Physics Series, Vol. LXXXV (Wiley, New York, 1994), pp. 733–773.

[9]M. G. Kozlov, ''Faraday effect in strong laser field,'' Opt. Spectrosc. (USSR) **67** (6), 789–792 (1989) [Russian original: Opt. Spektrosk. **67** (6), 1342–1345 (1989)]; K. P. Zetie, R. B. Warrington, M. J. D. Macpherson, D. N. Stacey, and F. Schuller, ''Interpretation of nonlinear Faraday rotation in samarium vapor,'' Opt. Commun. **91** (3-4), 210–214 (1992).

[10]B. Schuh, S. I. Kanorsky, A. Weis, and T. W. Hänsch, ''Observation of Ramsey fringes in nonlinear Faraday rotation,'' Opt. Commun. **100** (5-6), 451–455 (1993). This approach was also independently suggested in D. Budker, D. DeMille, E. D. Commins, and M. Zolotorev, ''Nonlinear optical rotation in separated laser fields and its application to the search for P and T violation,'' 17 pp., 1992 (unpublished).

[11]S. I. Kanorsky, A. Weis, and J. Skalla, ''A wall-collision-induced Ramsey resonance,'' Appl. Phys. B: Lasers Opt. **60** (2-3), S165–S168 (1995).

[12]A. Weis, J. Wurster, and S. I. Kanorsky, ''Quantitative interpretation of the nonlinear Faraday effect as a Hanle effect of a light-induced birefringence,'' J. Opt. Soc. Am. B **10** (4), 716–724 (1993); S. I. Kanorsky, A. Weis, J. Wurster, and T. W. Hänsch, ''Quantitative investigation of the resonant nonlinear Faraday effect under conditions of optical hyperfine pumping,'' Phys. Rev. A **47(2)**, 1220–1226 (1993).

[13]D. Budker, V. Yashchuk, and M. Zolotorev, ''Nonlinear magneto-optic effects with ultra-narrow widths,'' Phys. Rev. Lett. **81**(26), 5788–5791 (1998).

[14]L. M. Barkov, M. S. Zolotorev, and D. Melik-Pashayev, ''Amplification of a $(P+T)$-odd optical activity,'' Sov. JETP Pis'ma **48** (3), 144–147 (1988) [Russian original: Pis'ma v Zh. Eksp. Teor. Fiz. **48** (3), 134–138 (1998)].

[15]I. B. Khriplovich and S. K. Lamoreaux, *CP Violation without Strangeness. The Electric Dipole Moments of Particles, Atoms and Molecules* (Springer-Verlag, New York, 1997).

[16]S. E. Harris, ''Electromagnetically induced transparency,'' Phys. Today **50** (7), 36–42 (1997).

[17]E. Arimondo, ''Coherent Population Trapping in Laser Spectroscopy,'' in

Progress in Optics XXXV, edited by E. Wolf (Elsevier Science B.V., New York, 1996), pp. 259–354.
[18]S. Brandt, A. Nagel, R. Wynands, and D. Meschede, ''Buffer-gas-induced linewidth reduction of coherent dark resonances to below 50 Hz,'' Phys. Rev. A **56** (2), R1063–R1066 (1997).
[19]M. Fleishhauer and M. O. Scully, ''Quantum sensitivity limits of an optical magnetometer based on atomic phase coherence,'' Phys. Rev. A **49** (3), 1973–1986 (1994).
[20]M. Faraday, *Experimental Research in Electricity* (Richard Taylor and William Francis, London, 1855), Vol. III, entries 2152, 2164.
[21]D. Macaluso and O. M. Corbino, ''Sopra Una Nuova Azione Che La Luce Subisce Attraversando Alcuni Vapori Metallici In Un Campo Magnetico,'' Nuovo Cimento **8**, 257–258 (1898); ''Sulla Relazione Tra Il Fenomeno Di Zeemann E La Rotazione Magnetica Anomala Del Piano Di Polarizzazione Della Luce,'' *ibid.* **9**, 384–389 (1899).
[22]There are different definitions of the terms ''alignment'' and ''orientation'' in the literature. For example, in R. N. Zare, *Angular momentum: understanding spatial aspects in chemistry and physics* (Wiley, New York, 1988), alignment designates even moments in atomic polarization (quadrupole, hexadecapole, etc.), while orientation designates the odd moments (dipole, octupole, etc.). We use the convention of E. B. Alexandrov, M. P. Chaika, and G. I. Khvostenko, *Interference of Atomic States* (Springer-Verlag, New York, 1993), in which alignment designates the second (quadrupole) polarization moment, and orientation designates the first (dipole) polarization moment.
[23]A. P. Kazantsev, V. S. Smirnov, A. M. Tumaikin, and I. A. Yagofarov, ''Effect of atomic ground state self-polarization in the optical-pumping cycle on the increase of linear light absorption for j to $j+1$ transitions,'' Opt. Spectrosc. **57** (2), 116–117 (1984) [Russian original: Opt. Spektrosk. **57** (2), 189–191 (1984)].
[24]A. Corney, *Atomic and Laser Spectroscopy* (Clarendon, Oxford, 1988), Chap. 15.
[25]The separation of the nonlinear Faraday effect into the hole-burning and the coherence contribution appears very useful in understanding the underlying physical mechanisms of the phenomenon, and in determining the widths of the magneto-optical resonances (Ref. 7). The two contributions are closely related, however, since they both originate from optical pumping. Thus, unified theoretical treatments of these effects are possible (Ref. 9), which are in good agreement with experiment (Ref. 7).
[26]Environmental Optical Sensors, Inc., Boulder, CO 80301-3376, phone: (303) 530-7785, http://www.eosi.com. The EOSI 2010 system has a built-in wavemeter. After initial calibration, it can display absolute wavelength with uncertainty of ± 0.1 nm, which is more than adequate to place the laser frequency within a smooth electronic tuning range from an atomic resonance.
[27]Stanford Research Systems, Sunnyvale, CA 94089, phone: (408) 744-8040, http://www.srsys.com.
[28]National Instruments, Austin, TX 78730-5039, phone: (512) 794-0100.
[29]S.-. Kim, S.-E. Park, H.-S. Lee, C.-H. Oh, J.-D. Park, and H. Cho, ''High-resolution spectroscopy of rubidium atoms,'' Jpn. J. Appl. Phys., Part 1 **32**, 3291–3295 (1993); O. Schmidt, K.-M. Knaak, R. Wynands, and D. Meschede, ''Cesium saturation spectroscopy revisited: How to reverse peaks and observe narrow resonances,'' Appl. Phys. B: Lasers Opt. **59** (2), 167–178 (1994); I. M. Beterov, I. I. Ryabtsev, V. M. Entin, and V. B. Elman, ''Alignment in Doppler free spectroscopy of ^{87}Rb,'' ICAP 16 Abstracts, Windsor 1998, p. 345; W. K. Hensinger, A. G. Truscott, H. Rubinsztein-Dunlop, and N. R. Heckenberg, ''Variations of relative line intensity in saturation spectroscopy due to low magnetic fields,'' submitted to Opt. Quantum Electron.
[30]This cell was manufactured in the early sixties and is a leftover from the intense investigations of optical pumping carried out at UC Berkeley at that time; see, e.g., J. Yellin, Ph.D. thesis, UC Berkeley, 1965; H. M. Gibbs, Ph.D. thesis, UC Berkeley, 1965. Coated (and uncoated) cells are also available commercially, e.g., from EOSI, Boulder, CO.
[31]E. Pfleghaar, J. Wurster, S. I. Kanorsky, and A. Weis, ''Time of flight effects in nonlinear magneto-optical spectroscopy,'' Opt. Commun. **99**, 303–308 (1993).
[32]M. A. Bouchiat and J. Brossel, ''Relaxation of Optically Pumped Rb Atoms on Paraffin-Coated Walls,'' Phys. Rev. **147** (1), 41–54 (1966).
[33]E. B. Alexandrov, M. V. Balabas, A. S. Pasgalev, A. K. Vershovskii, and N. N. Yakobson, ''Double-Resonance Atomic Magnetometers: from Gas Discharge to Laser Pumping,'' Laser Phys. **6** (2), 244–251 (1996).
[34]C. Wieman and T. W. Hänsch, ''Doppler-free laser polarization spectroscopy,'' Phys. Rev. Lett. **36**, 1170–1173 (1976).
[35]Channel Industries, Inc., tel. (805) 967-0171, change in length type tube, wall thickness 20 mills, material type C-5600.
[36]Magnetic Shield Corp. Perfection Mica Company, Bensenville, IL 60106, tel. (630) 766-7800.

THE CRUEL PESSIMISM OF SCIENCE

The official, popularizing versions of the story [of science], written by scientists or philosophers like Bertrand Russell who allowed themselves to be seduced by science, are very different from mine. For them the story is heroic, a great human struggle to free ourselves of the shackles of old illusions and confront the one certain truth that it is our particular destiny to grasp. Science, in this view, is a triumphant human progress towards real knowledge of the real world. This is the official view of the schoolroom and the television spectacular. For me it is nonsensical propaganda which conceals all the important issues. In my version the story is a sad one, a long tale of decline and defeat, of a struggle to hold back the cruel pessimism of science.

Bryan Appleyard, *Understanding the Present—Science and the Soul of Modern Man* (Pan Books, London, 1992), p. 79.